LEAD-LAG DYNAMICS OF A ROTOR WITH STICK-SLIP NONLINEARITY

Philipp Andersch and Manfred Hajek
Institute of Helicopter Technology
Technische Universität München, Germany
andersch@tum.de

Abstract

An assessment of a frictional helicopter blade attachment with regard to its influence on the dynamics of the in-plane blade motion is presented. For detailed system analysis, a 3D finite element model with contact modeling has been created and validated using preexisting test data. Using the insights gained from 3D finite element simulations, a reduced order model suitable for dynamical simulations is derived and parameterized. Eventually, the reduced order model for the blade attachment is inserted into a hingeless dynamical rotor model with elastic coupling. The influence of the blade attachment on lead-lag dynamic behavior is investigated using the developed model and multiple configurations are compared to each other to identify the effects of the nonlinear blade attachment model on lead-lag frequency and damping ratio as well as elastic coupling prevalent in the hingeless rotor configuration.

NOTATION

FE	Finite element
ROM	Reduced order model
DoF	Degree of freedom
θ	Collective blade pitch angle

1 INTRODUCTION

Helicopter flight mechanics – and even more so – helicopter blade dynamics are strongly dependent on the way a blade is attached to the rotor hub. Nonlinearities in this part may present serious challenges for rotordynamicists as they may have a severe impact on the overall system behavior[13]. However, in order to achieve compact and lightweight designs, many helicopter rotor configurations incorporate nonlinear components at the blade root. Nonlinearities influencing the lead-lag motion of a helicopter blade in particular may arise from multiple sources. Elastomeric dampers exhibit nonlinear hysteretic behavior and the effects on blade dynamics have been investigated in Gandhi and Chopra[4]. Muscarello and Quaranta[9] describe a nonlinear hydraulic lead-lag damper causing limit cycling of a helicopter ground resonance model. Bauchau et al.[1] have analyzed the use of semi-active friction dampers where the contact normal force is used to improve dynamical blade behavior.
Nonlinear blade behavior can also result from the way a blade is attached to the rotor hub. The EC145, for example, uses a glass fiber reinforced plastics loop in a metallic casing to transfer blade loads to the rotor hub. The basic setup of such a rotor is depicted in Fig. 1. The blade (1) forms a loop which is held by two casings (2) connected with bolts of which the upper one is not shown. This arrangement is attached to the mount (3) which is pivoted in the rotor head (4) and may rotate to control the blade pitch angle. The arrangement features a pitch bearing but lacks flap and lag hinges and is thus classified 'hingeless'. Flapping and lagging motion of the blade in flight may occur by means of elastic blade bending. The blade may be considered as a cantilevered beam and bending will

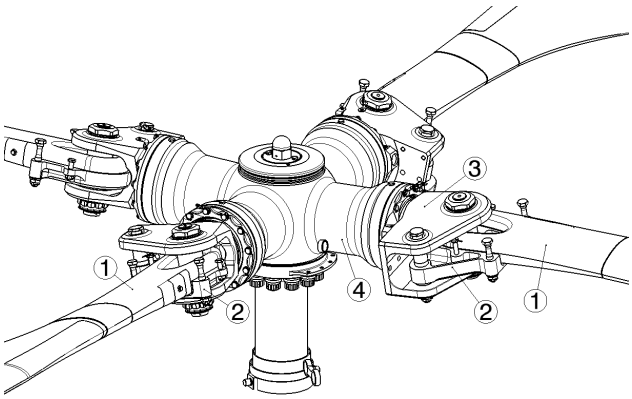

Figure 1: Hingeless rotor design with loop-type blade attachment

occur in the blade root region shown in the lower right corner of Fig. 1. Clearly, the dimensions of the blade root are not equal in the plane of the loop and perpendicular to that. This means, that depending on the pitch angle of the blade different bending stiffnesses will be effective for in-plane and out-of-plane motion of the blade.
The loop-type attachment is known to be not completely rigid. Moreover, the loop will slide when high in-plane bending moments occur and the frictional forces are assumed to provide additional damping – a feature that has allowed helicopters with this rotor design to operate without dedicated lead-lag dampers. This stick-slip element further complicates rotor dynamic analysis since it produces a strong interplay between the deformation of the blade and the component state. Elastic blade deformation (e.g. blade mode shapes) is modified by changing boundary conditions and the bending moments at the blade root in turn determine the frictional forces at the loop. The approach followed in this paper is to derive a reduced order model for a loop-type blade attachment and to introduce this into a rotor model for integrated dynamical simulation (strong coupling).
The analysis of rotor dynamics requires complex aeromechanical models. Some advanced rotorcraft analysis codes have been developed and constitute the standard in academia and industry. CAMRAD II[7], for example, offers model analysis using its trim, flutter and transient task. Rotor trim is efficiently obtained by harmonic solutions methods, the flutter task performs linear system dynamic analysis and the transient task can be used to compute trajectories in the time domain. Hard nonlinearities like stick - slip friction may have a significant effect on the blade's dynamics but these effects cannot be analyzed through linearization. Analysis can be conducted in the time domain, but switching systems are a major challenge for numerical solvers[1]. In Muscarello and Quaranta[9] the describing function method is used to conduct a stability analysis for a helicopter ground resonance model with nonlinear lead-lag dampers in the frequency domain.
This paper presents the development of a rotor model using the Modelica language in conjunction with the Dymola software which allows efficient formulation of dynamical systems featuring nonlinearities like stick-slip friction[3]. Dynamic analysis of an elastically coupled hingeless rotor design is conducted in the time domain once hard nonlinearities are included into the model.

2 BUILDING THE ROTOR MODEL

2.1 Flexible blade formulation

Flexible blade modeling is based on the beam theory described by Johnson[7]. The nonlinear finite element beam formulation has been implemented in Modelica and extensively tested by Spieß[12]. The method of a floating frame of reference is applied and geometrical nonlinearities up to second order as well as structural cross couplings typical for helicopter rotor blades are accounted for.

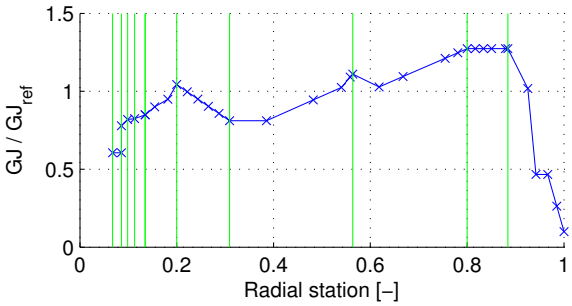

Figure 2: Torsional rigidity over blade span

2.2 Aerodynamics

Aerodynamic forces are obtained by blade element theory for a finite number of blade elements. The aerodynamic forces act via structural dynamic interfaces on the beam element leading to dynamic blade deformation. To model rotor inflow for dynamical analysis such as ground resonance, it has been shown[2][6] that inflow dynamics have to be considered. The dynamic inflow model of Pitt and Peters[11] has been implemented into the simulation environment according to the formulation given in Peters and HaQuang[10]. However, since this analysis only considers the blade dynamics for a fixed rotor hub with zero cyclic pitch in hover the model is reduced to a single blade coupled with a uniform inflow model.

2.3 Rotor model fidelity

The sample rotor model used for the analysis in this paper features sufficient details of an industrial rotor design demonstrating that the developed code is able to handle rotor models of realistic complexity. The 15 structural parameters necessary for the structural dynamic beam components are given at 42 radial stations of the blade. Due to the ability of the beam formulation to incorporate linearly varying structural properties, the rotor blade can be represented by using a significantly reduced number of beam elements. To illustrate the complexity of the structural dynamical parameterization the torsional rigidity of the blade assembly is displayed in Fig. 2. The torsional rigidity changes moderately within the beam elements marked by the vertical lines except for the blade tip. That is why the flexible degrees of freedom are removed for the tip element and a rigid body element is used instead.
To limit the computational burden a study has been

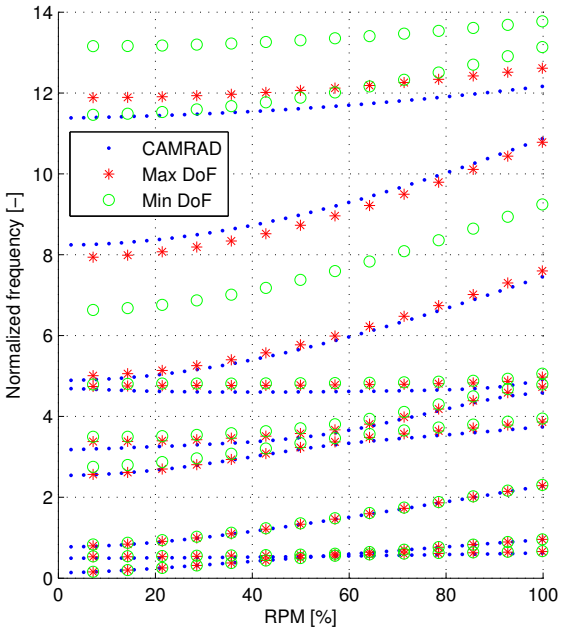

Figure 3: Comparison of natural frequencies over rotational speed for a blade in vacuo

conducted on how many elements are necessary to capture the principal blade dynamics and it has been shown that nine flexible beam elements are sufficient to predict the dynamical blade behavior necessary for lead-lag analysis.

According to the number of shape functions used, the total number of degrees of freedom (DoF) of the model may be varied. Figure 3 shows Campbell's diagram using two configurations for the structural dynamic model as well as the results from the reference model. The first configuration features 14 DoF for every flexible beam element (four extension, three bending in-plane, three bending out-of-plane and four torsion) while the second configuration only employs four DoF for every flexible beam element (one shape function for each category of physical deformation). Therefore, the model with the minimum amount of shape functions has 36 DoF in total and the model with the maximum number of shape functions already features 126 DoF. Results are compared to the results of modal analysis of a corresponding CAMRAD model. It can be deduced that the fidelity of the model can be enhanced by using more shape functions. However, the model with only 36 DoF is seen to suffice for low-frequency dynamic analysis. Mode shapes from the reference CAMRAD model and the Modelica model with less DoF at nominal rotor speed are compared in Fig. 4 and it is observed that the fundamental modes of the blade assembly agree. Structural damping is chosen to be very moderate.

The airfoil in the presented simulation model consists of 24 radially distributed segments with individual chord length and the aerodynamic forces are determined via linear interpolation, using the local blade element data as input. A visualization of the rotor model is shown in Fig. 5. Tuning masses (red) are attached to the elastic beam elements (green). The airfoil is not shown but the discrete airloads are displayed as vectors acting on the respective blade sections and approximating a continuous airload distribution.

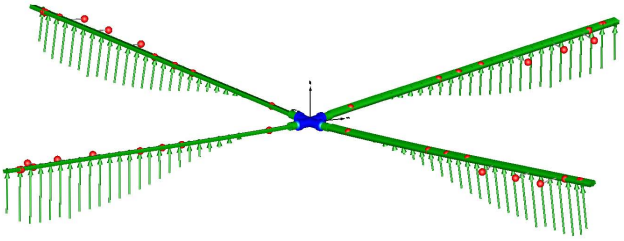

Figure 5: Rotor model visualization

3 NONLINEAR BLADE ATTACHMENT

3.1 Component test and model

Preexisting data has been used to set up and parameterize a 3D finite element model of the loop attachment in ANSYS. The geometry of the attachment is shown in Fig. 6.

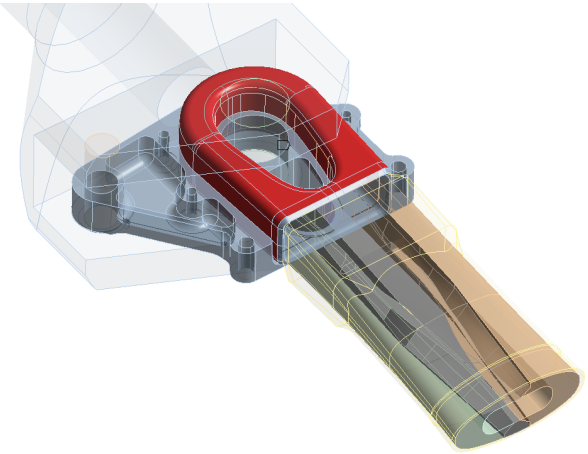

Figure 6: Geometry of 3D finite element model

The model consists of the following elements:

- Mount for component experiment [not fully shown, transparent]
- Titanium loop casing (upper [not displayed] and lower [shown in gray]), attached to the mount using two bolts
- Blade root (various materials) and glass fiber loop [highlighted in red] in frictional contact with metallic casing

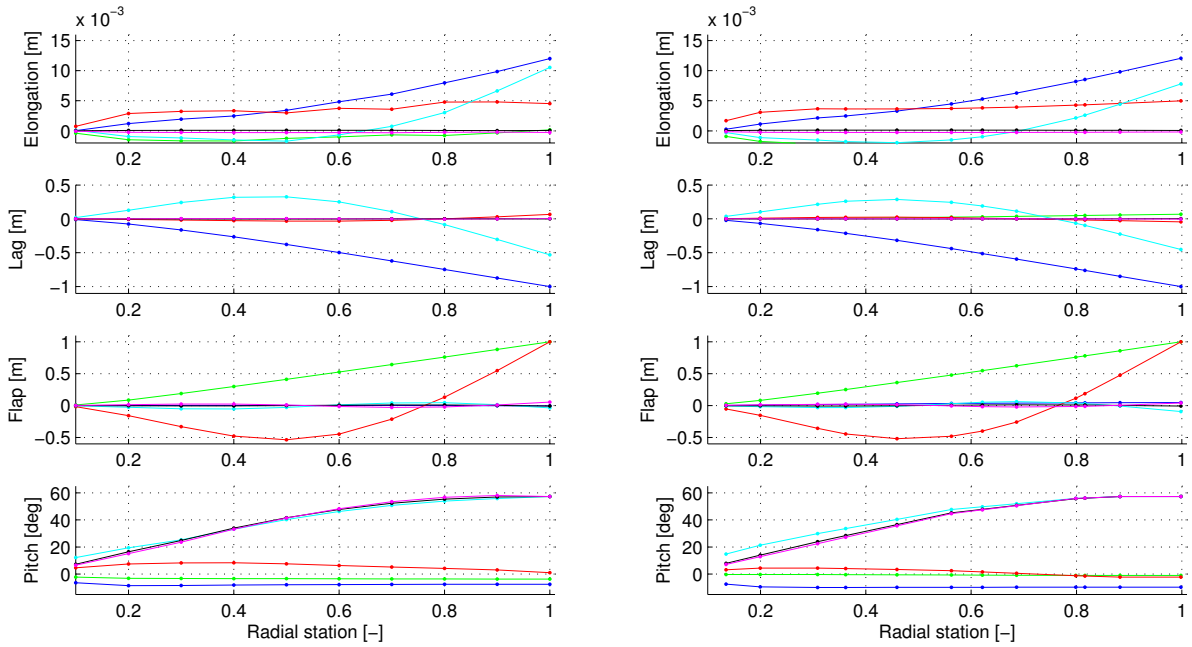

(a) CAMRAD II model

(b) Modelica model

Figure 4: Comparison of mode shapes for a blade at nominal rotational speed in vacuo

To model stick-slip contact, the model employs ANSYS' CONTA174 contact element in combination with a simple Coulomb friction model. The component test is conducted with a 1.6 m long blade sample which is reinforced and connected to hydraulic actuators at its outward station. A large axial force is applied in order to simulate centrifugal forces arising in flight condition. Furthermore, the hydraulic actuators allow a displacement-controlled loading of the structure in lead-lag, flapping and even torsional direction. A reference trajectory where only a zig-zag displacement profile in lag direction is applied is chosen to compare test data and simulation results.

As shown in Fig. 6 the FE model does not incorporate the whole mechanical setup. The blade is modeled up to a distance of 0.35 m from the main bolt used to connect the casings to the mount. There, the structure is cut and the surface nodes of the cut area are coupled with a single node which is used to apply cut forces and torques leading to similar load conditions as in the component test.

To parameterize the model the bending moment at the mount was considered. Due to curing of the composite material, an initial gap between the fibre loop and the casing is produced. A thermal load on the loop is used in the ANSYS model to control the gap width. The bending moment observed at the mount turned out to be very sensitive to the temperature load (gap width respectively), the coefficient of friction applied and the exact coordinates of the node used to apply the cutting forces and torques. The latter is due to the high axial loading, which produces significant changes in the estimated bending moments for small variations of the lateral node coordinate. As a consequence, the temperature loading, the coefficient of friction as well as the node coordinates where chosen such that the bending moment at the mount was closely predicted by the simulation results for all loadsteps along the reference trajectory.

Due to friction, a back and forth motion trajectory produces a hysteretic behavior when the bending moment is plotted over travelled actuator distance. Results from the simulation as well as test data are shown in Fig. 7. Hysteresis is very moderate and hardly observable for this physical quantity.

During the experiment, data was recorded from additional strain gauges on the upper and lower surface of the blade root. These elastic strains from the simulation and the test data show good agreement substantiating the 3D finite element model fidelity.

3.2 Deriving a reduced order model for the blade attachment

To study how the described blade attachment influences dynamical blade behavior, a reduced order model (ROM) for the blade root is developed. As the loop sliding only has major effects on the in-plane motion of the blade the reduced order model is derived focusing on this kind of movement. For this part, the test rig mount is excluded from the model and zero displacement boundary conditions are applied to the

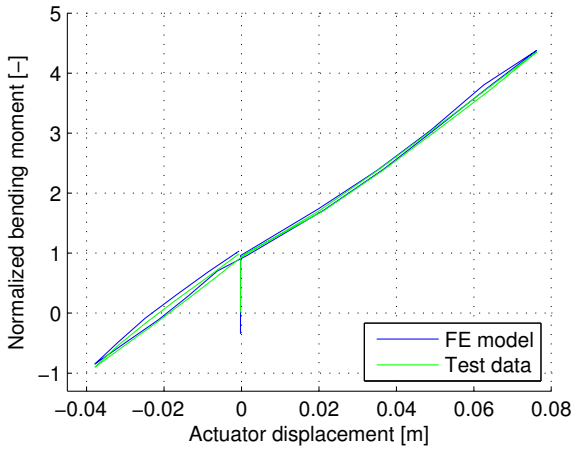

Figure 7: In-plane bending moment at mount over traveled actuator distance under high axial loading

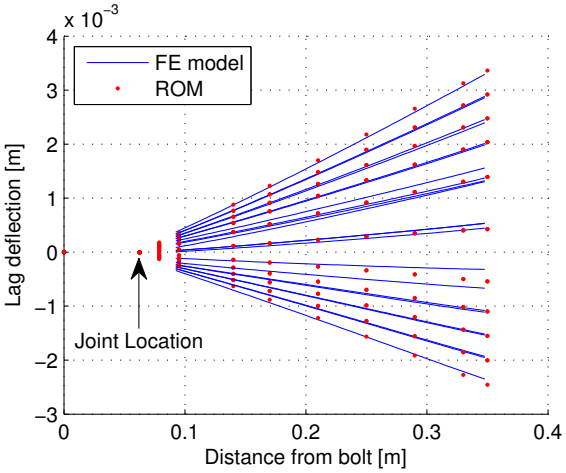

Figure 9: Deflection of blade root as obtained from FE model and ROM without friction for high axial and zig-zag in-plane load

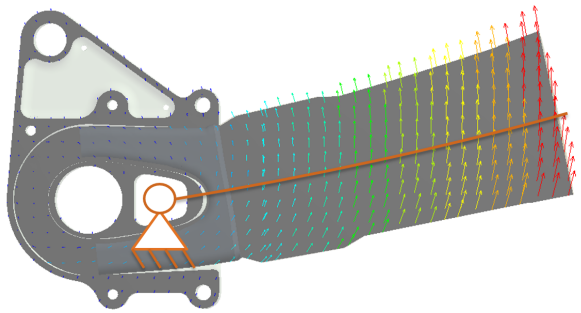

Figure 8: Reduced order model kinematics and deformation plot obtained with ANSYS

bolt holes of both casings.

From simulations conducted with the FE model it can be observed that the loop deformation for in-plane bending can be approximated by a rotation of the blade around a fixed point. This point is estimated from deformation plots. In addition to this rotation the blade root also exhibits elastic deformation. The kinematics of the blade attachment are therefore approximated using a fixed revolute joint with attached beam elements. The structure of the reduced order model is shown in orange superimposed on a deformation plot of the FE model with highly exaggerated deformations for visual inspection in Fig. 8.

After settling on a kinematic representation of the ROM, the model needs to be augmented and parameterized to adequately represent the blade attachment. Nominal stiffness values for the blade root were kept and used to parameterize the structural properties for the four beam elements representing the flexible blade root. The loop part of the blade attachment is represented by the revolute joint, which is augmented with a nonlinear spring and Coulomb friction elements. Using the finite element model, it was possible to parameterize these characteristics independently.

In a twofold approach the stiffness properties are parameterized first. To this aim, a simulation along a suitable load trajectory was performed using a contact model without friction. The high axial force from the previous simulations was kept and only a zig-zag load history for the lateral force was chosen. The nonlinear spring at the revolute joint of the ROM was parameterized for best agreement of the deflection curve of the blade root extracted from the FE model and the deflection of the ROM at discrete locations, shown in blue and red respectively in Fig. 9. The assumption on the reduced order model kinematics is best verified here. Although slight deviations can be noted the overall representation of the deflection curve by the reduced order model is considered sufficient.

Figure 10 shows the lateral force – displacement relationship for the point at which the loads attack for the FE model and the ROM. Clearly, a stiffening of the structure for higher loads is observed. This is not only due to the restoring moment from the axial load but also caused by the loop deformation characteristics. The nonlinear spring used in the ROM features higher stiffness for large angles of the revolute joint, thus it will produce a behavior similar to backlash.

Secondly, the effects of loop friction shall be considered. The same load trajectory as above is applied to the model, now taking into account frictional forces. In this case the deflection assumed by the system becomes dependent on the load history as the deflection curves for the loading and unloading part of the load trajectory no longer coincide. Consequently, the lateral force - displacement relationship shown in Fig. 11 b forms a hysteresis. A load trajectory with smaller and larger amplitude (Figs. 11 a and 11 c respectively) have been applied to both models to check how well the model scales with amplitude.

The setup of the reduced order model is shown in

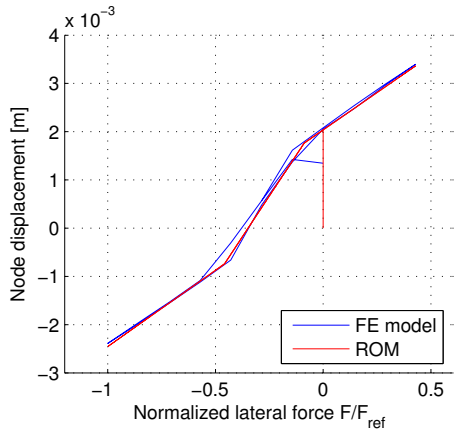

Figure 10: Force and displacement for outer node under high axial and zig-zag in-plane load, obtained using the model without friction

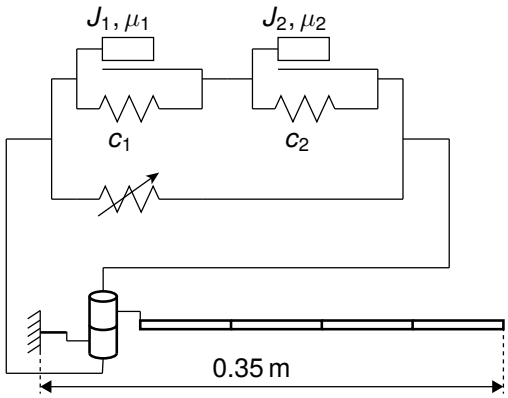

Figure 12: Setup of the reduced order model

Fig. 12. The model features a so-called Iwan model consisting of two discrete Coulomb elements coupled with linear springs. By connecting multiple discrete Coulomb elements in the shown way, the smooth hysteresis produced by a continuous frictional surface can be approximated[8]. With different frictional coefficients μ_i and different spring constants c_i one discrete element may slide while the other may stick in certain modes of operation. Using adequate parameters, the shape of the resulting hysteresis may be designed. The Iwan model is connected to the revolute joint with the nonlinear spring in a parallel arrangement. With four beam elements (4 DoF each) and two discrete Coulomb friction elements the model for the blade root has 18 degrees of freedom in total.

4 METHODOLOGY FOR DYNAMICAL ANALYSIS AND VALIDATION

In order to adequately assess blade dynamics when hard nonlinearities are present, the blade tip trajectory in the time domain is used to estimate modal parameters. An in-plane force is applied to the blade tip and an equilibrium state of the system is obtained through time marching integration. The step-like removal of the load produces oscillatory blade motion. This trajectory is well-suited to study the dynamical behavior of the lead-lag motion in particular. For a defined force applied to the blade tip, the oscillatory trajectory is recorded for about three periods and subsequently used for the estimation of the motion frequency and damping. Three periods are chosen because the damping ratio can be determined reliably. At the same time, it is important to constrain the length of the oscillation signal used for modal parameter estimation. If modal parameters are identified for a substantially longer oscillation signal, the effects of motion amplitude dependency will not show up for many operating conditions. The characteristic frequency of the witnessed lead-lag motion is obtained by Fast Fourier Transform and the damping can be determined using the method of logarithmic decrements.

As a proof of concept, the dynamics of a baseline rotor blade without hard nonlinearities are assessed in this section. The reference model is an ideal bearingless helicopter rotor where flapping and lagging occur only by means of elastic blade bending. For this model without hard nonlinearities the modal parameters (normalized frequency and normalized damping ratio) obtained as described above are compared to the modal parameters obtained from an eigenvalue analysis after linearization in Fig. 13. It can be concluded that it is possible to extract the modal parameters for the fundamental lead-lag motion from the blade oscillation in the time domain using the described excitation.

For higher collective angles a slight drop in oscillation frequency is observed. This is easily explained by the fact that the blade root stiffness in the airfoil direction of the blade is approximately six times higher than the one perpendicular to the airfoil. The rotor under consideration does therefore not belong to the class called 'matched stiffness' rotors. As the blade root is pitched, the in-plane motion is more and more a consequence of root bending about the elastic axis with lower bending stiffness. The increase in damping for higher blade pitch angles θ is due to the fact that the inclined airfoil supplies more aerodynamic damping than is available from sole profile drag.

As the whole blade is inclined to alter collective pitch, the fundamental mode shape changes. Figure 14 shows the mode shapes of the blade obtained through linearization in the trim state for different collective pitch angles, all of them normalized to the same lag deflection at the blade tip. Clearly, for a collective pitch of 11°, almost no flapping motion occurs and for a collective angle of 20° the fundamental mode involves most out-of-plane motion. The sign of the lag-flap coupling changes from collective angles of 8° to 20°. This change in mode shape is also observed when the trajectory of the blade tip is recorded in the time domain

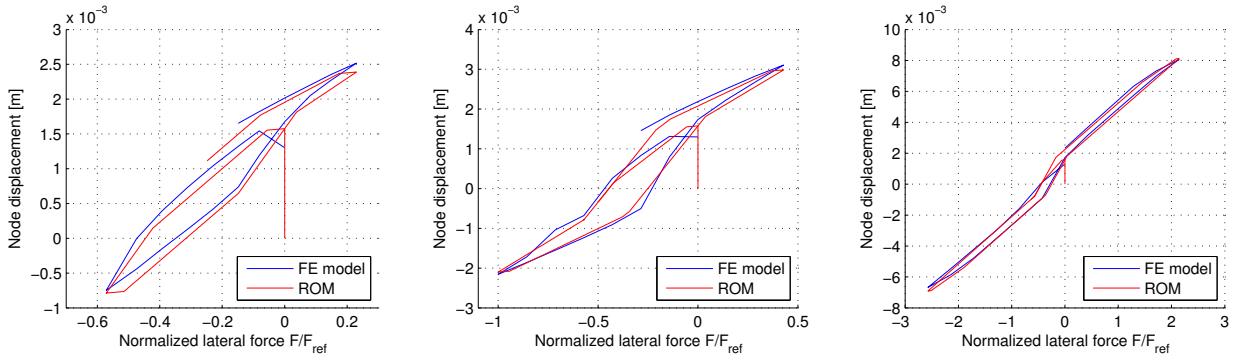

(a) Small amplitude **(b)** Medium amplitude **(c)** Large amplitude

Figure 11: Force and displacement for outer node under high axial and zig-zag in-plane load with three different amplitudes, obtained using the model with friction

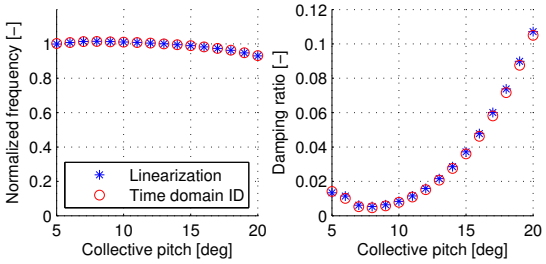

Figure 13: Comparison of results for elastic blade lead-lag dynamics, obtained by linearization and from time domain response

(Fig. 15), supporting the approach to derive modal parameters from the oscillation curve which is clearly dominated by the mode of interest. The method of analyzing the oscillatory blade tip curves will be applied to the model augmented with the hard nonlinearity in the following section 5, since for this system no valid conclusions can be drawn from pure linearization.
The described change in flap-lag coupling is also described[5] for the MBB Bo105 rotor, a rotor design similar to the one under consideration here.

5 ANALYSIS

The analysis compares dynamical properties for five blade setups:

1. Lin - baseline model (nominal stiffness, clamped blade)
2. Mod - augmented model with complete reduced order model
3. ModNoFrict - partially augmented model (nonlinear stiffness, without friction)
4. ModLinStiff - partially augmented model (linear stiffness equal to soft regime of ROM stiffness, with friction)

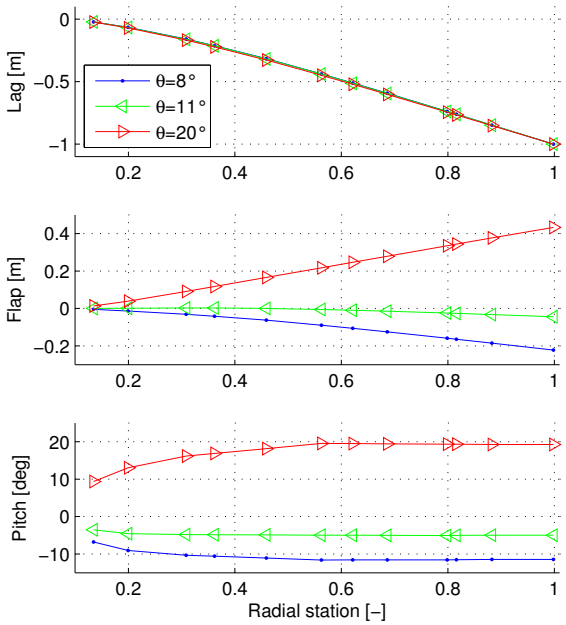

Figure 14: Fundamental mode shape for the baseline model with different collective pitch angles

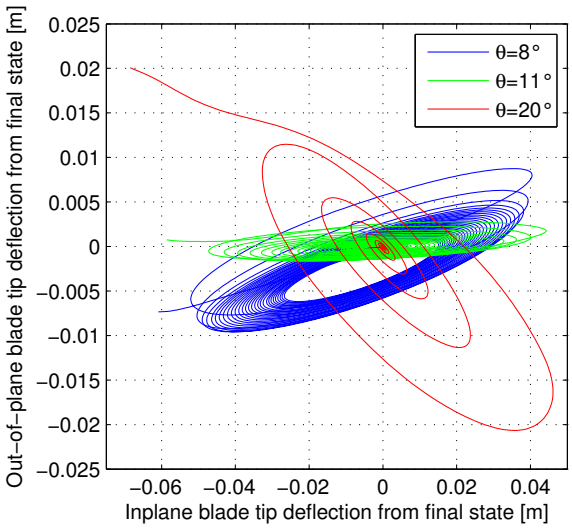

Figure 15: Tip displacements from final state for baseline model oscillations

5. Lin2 - baseline model with reduced stiffness in the direction of the airfoil at the blade root. The stiffness reduction is chosen such that frequencies for this model and the one featuring the reduced order model are comparable.

5.1 Change in oscillation mechanism

For the augmented model linear modal reduction is no longer viable. To examine the couplings prevalent in the modified blade configuration, three different trim states are obtained using a model where the frictional part at the joint is removed but which still features the nonlinear spring and the revolute joint. Figure 16 a shows the fundamental mode shape for the model in its respective trim state and Fig. 16 b shows the fundamental mode shape when the joint is locked after the trim state has been computed (equivalent to an operating state where the ROM remains in sticking). Again, both mode shapes are normalized to a unit deformation in the in-plane direction. It can be concluded, that for all three considered trim conditions the lag-flap coupling for the considered mode is reduced by the introduction of the additional lag joint within the reduced order model. This was expected since the joint reduces structural stiffness in the direction of the airfoil, alleviating the great difference in blade root bending stiffness for both elastic axes of the baseline model addressed in section 4. The mode shapes shown in Fig. 16 b and Fig. 14 are similar but not identical as long as the same collective pitch angle is considered. The only difference in the system is a sweep angle introduced by the locked joint according to the respective trim condition. The sweep angle assumed by the system before locking is tabulated in Table 1.

For small amplitudes of motion the augmented model

Collective pitch angle	Sweep angle
8°	0.5089°
14°	0.0456°
20°	-0.5152°

Table 1: Static sweep angle due to locking joint for different trim conditions

with the full ROM will remain in sticking for larger shares of the the lead-lag oscillation period. Because of the changes in linear mode shapes demonstrated by Fig. 16 it is questionable, if elastic coupling is more pronounced in these cases. In Fig. 18, the elastic coupling is analyzed for the model with friction and nonlinear stiffness in terms of the blade tip movement for small and large amplitude motion. Also shown are the joint angles of the blade attachment ROM, where for small amplitude motion, phases of sticking can be identified. The dashed lines mark the region of reduced stiffness, similar to backlash.

To compare trajectories, the blade tip movement is shown with appropriate scales. However, the ratio between the scale of the in-plane motion and the out-of-plane motion is kept constant. The trajectories demonstrate that for the smallest examined motion amplitude the short sticking phases do not produce a completely different elastic coupling when compared to a trajectory where almost no sticking occurs. This holds for the limited trajectory used for modal parameter estimation of three periods as outlined in section 4. With reference to Fig. 15, it can be concluded that lag-flap coupling is severely reduced by introducing the proposed model for the blade attachment.

The effect of a considerable change in the oscillation mechanism can also be demonstrated using the presented models but is limited to very small amplitudes. Figure 17 shows the blade tip trajectory for the model with friction and linear soft stiffness as well as the corresponding motion of the joint subject to friction. Starting from initially small oscillation amplitudes, after four periods the amplitude of the oscillation has decayed to a level where the joint remains in sticking. From the blade tip trajectory it can be deduced that from this event on the trajectory changes towards higher lag-flap coupling. This observation agrees with what was inferred earlier in this section when mode shapes of the blade with free joint and locked joint were compared in Fig. 16. As a matter of fact, the trajectory takes on a steeper path after each turning point even before the joint completely ceases to move, a property that may be attributed to short phases of sticking. The described effect is most pronounced for the frictional model with linear soft stiffness but can also be found in the blade model featuring the full ROM. For both models, severe changes in elastic coupling only occur for very small amplitudes of motion. The blade tip trajec-

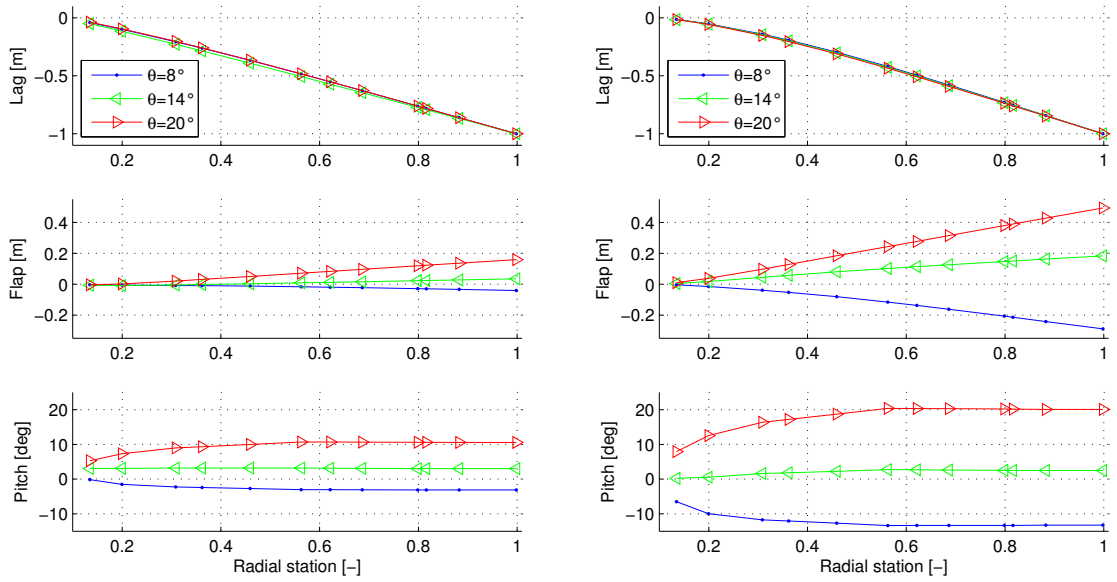

(a) Rotating joint

(b) Locked joint

Figure 16: Comparison of the fundamental mode shape for the blade model with frictionless and with locked joint

tory shown in Fig. 17 exhibits distinct nonlinear system behavior in contrast to the trajectories obtained with the baseline model in Fig. 15, emphasizing the need for nonlinear system models and respective nonlinear analysis as the one presented here.

However, for the given parameterization sticking is found to occur only locally or for confined operating conditions. This is due to the low coefficient of friction, presumably caused by PTFE lubrication in the loop casing. Damping and frequency values are not provided for extremely small motion amplitudes in this analysis since results tend to become noisier for small amplitudes and numerical effects will truncate results.

5.2 Dynamical analysis results

This section discusses the frequencies and damping ratios of the oscillatory motion provoked by the step-like removal of an in-plane force. Simulations have been conducted for various parameters and results are shown for two representative values of the exciting force.

The results for oscillation frequency for small amplitudes (Fig. 19 a) shall be discussed first. The baseline model (designated 'Lin') oscillates with the highest frequency due to its high structural stiffness. Because of the great difference in structural stiffnesses in the direction of the airfoil and perpendicular, the frequency declines when collective pitch is increased.

The linear model with reduced bending stiffness (designated 'Lin2') exhibits lower oscillation frequency and the effect of decreasing frequencies for higher collec-

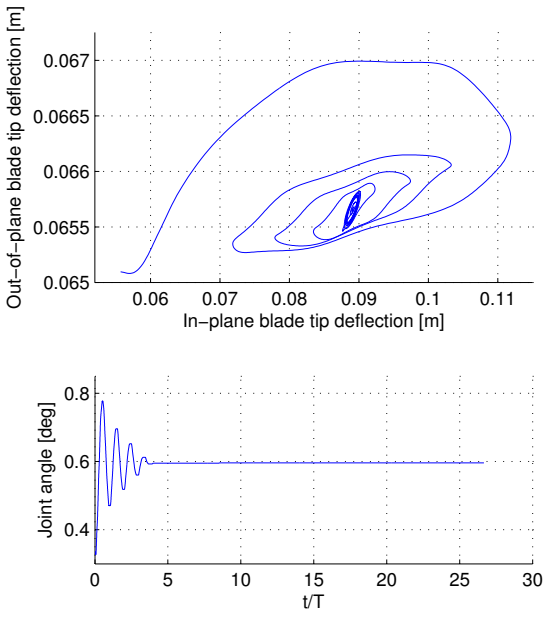

Figure 17: Oscillation trajectory for stick-slip model with soft linear stiffness and joint angle motion. Initial deflection from trim state corresponding to a collective pitch angle of 9° was achieved using a tip load of 150 N.

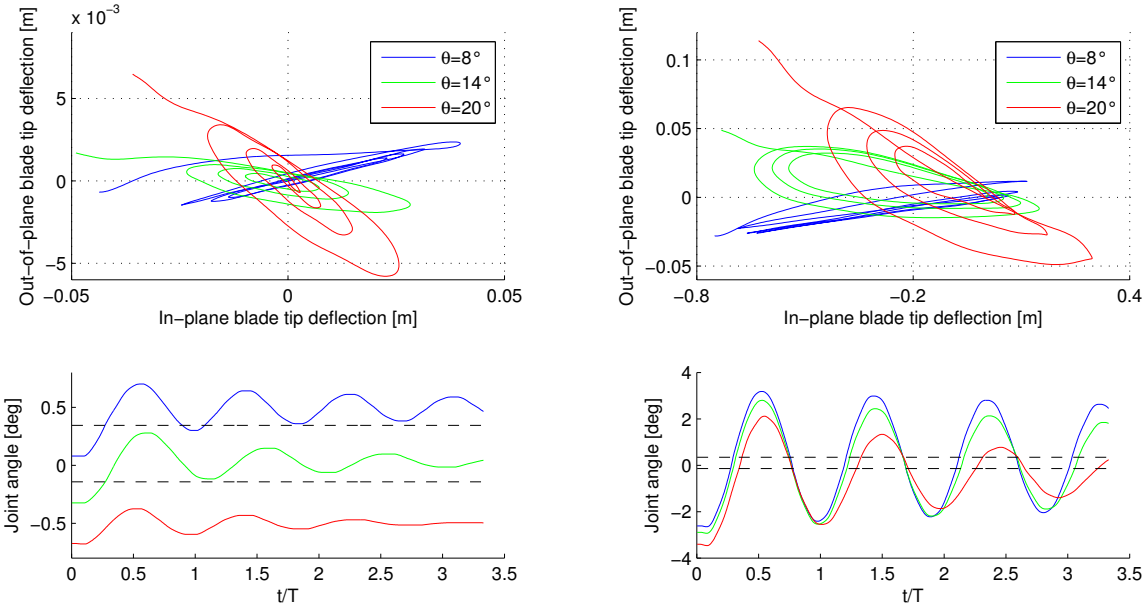

(a) Small amplitude motion (F=150 N) **(b)** Large amplitude motion (F=2500 N)

Figure 18: Elastic coupling for the fully augmented model in terms of blade tip displacement from final state for small and large motion amplitudes with respective joint motions indicating sticking phases. Dashed lines mark the region of reduced stiffness.

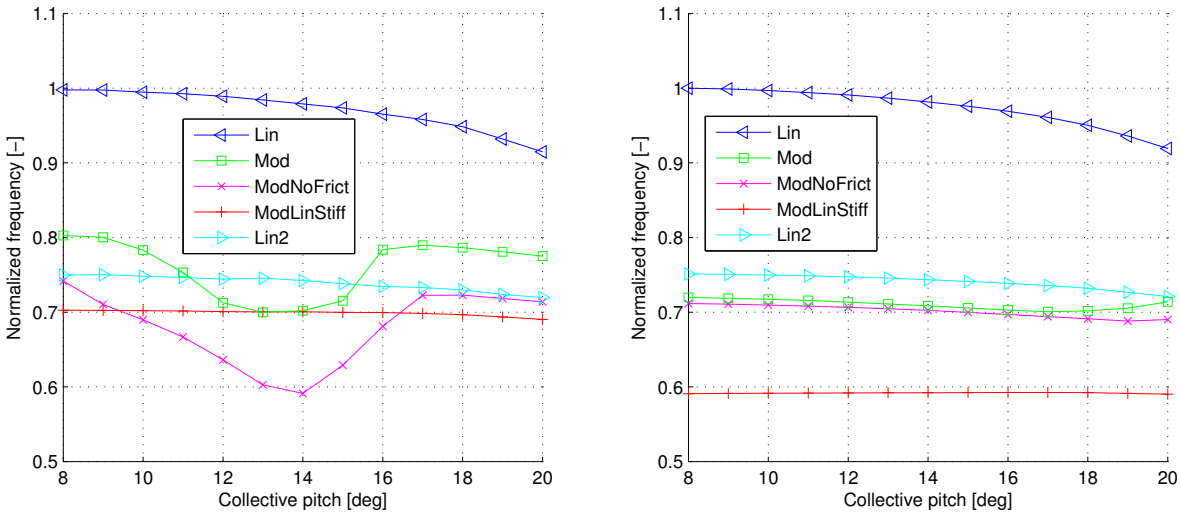

(a) Small amplitude motion (F=150 N) **(b)** Large amplitude motion (F=1000 N)

Figure 19: Oscillation frequency of the in-plane motion

tive pitch angles is still observable but less pronounced than for the baseline model (Lin).

The frequency of the model featuring the full ROM (designated 'Mod') is approximately in the same range as the one of the linear model with lowered bending stiffness (Lin2). However, from 12° to 15° collective pitch angle, a depression in oscillation frequency is identified. For these trim conditions, the nonlinear spring of the reduced order model stays in its softer regime for the most part of the witnessed oscillation due to the small amplitude of motion as can be seen in Fig. 18 a. For these operating conditions, the model with soft linear spring and friction (designated 'ModLinStiff') produces identical frequencies.

For the frictionless model with nonlinear stiffness (ModNoFrict), frequencies of small amplitude in-plane oscillation are constantly below the ones identified for the model with the full ROM (Mod). At this level of excitation, the frictional forces do have a considerable impact on the frequency of the lead-lag motion. Coulomb friction forces are saturated at a certain level and do not grow with motion amplitude in contrast to forces of linear damping models. For large motion amplitudes the frictional forces in the investigated model do not seem to have a relevant impact on the oscillation frequency since in Fig. 19 b it is shown that the models with and without friction (Mod and ModNoFrict) oscillate at the same frequency if stiffness properties match.

The models featuring neither friction nor the joint with nonlinear stiffness (Lin and Lin2) are considered linearizable and the oscillation frequencies remain independent of motion amplitudes as expected.

For the models with friction, frequencies are lower for large motion amplitude than for the small amplitude case in general. As far as the model with the full reduced order model (Mod) is concerned, there is no longer a region with noticeable change in frequency. Due to the larger motion amplitudes the spring no longer operates in either the soft or stiff regime but the soft region is crossed for a small fraction of the oscillation period as can be seen in Fig. 18 b.

Figure 20 a shows the identified damping ratio for the in-plane blade oscillation. Both linear models produce similarly lowly damped oscillations for low values of collective pitch angle. Damping ratios for the model featuring the full ROM (Mod) are increased by a factor of four. Highest damping is predicted for the configuration with friction and soft spring (ModLinStiff). For the operating region of a collective pitch angle between 12° and 15° this model describes the physics of the model with the full ROM as described above and indeed for this region the observed damping ratios correlate. For higher collective pitch angles damping increases due to an inclined airfoil as already discussed in section 4. However, the models with friction maintain their damping advantage also for higher angles of collective pitch.

For small and large motion amplitudes the identified damping ratio for both 'linear' models (Lin and Lin2) is the same as expected. Again, the models with friction show a motion amplitude dependent behavior. In agreement with what was observed for small motion amplitudes these models show higher damping when compared to the 'linear' models (Lin and Lin2) for small angles of collective blade pitch. The damping advantage is reduced though, but still considerable. The damping ratio of both models with friction is similar for all studied values of collective pitch for large motion amplitudes.

The damping ratio for both linear models is similar when small pitch angles are considered, for high pitch angles the baseline model (Lin) promises significantly higher damping than the model with reduced bending stiffness (Lin2), surpassing the damping of both models with friction for collective angles exceeding 16°. The divergence of the damping curves for both linear models is presumably due to more favorable elastic coupling for the baseline model: Again a lowered bending stiffness reduces the great difference in blade root bending stiffnesses in airfoil direction and perpendicular to it. This way, elastic coupling between lag and flap motion is reduced for the configuration with lower bending stiffness. According to Huber[5], this coupling constitutes a main source of damping for the in-plane motion.

Finally, very low values for damping are predicted for the frictionless model with nonlinear stiffness (ModNoFrict) independent from the amplitude of the considered motion, even ranging below the results obtained from both 'linear' models without the additional joint. At this point it is important to note that also for large motion amplitudes the frictional forces do have a considerable effect on damping as the damping ratio of both frictional models clearly ranges above the one for the frictionless model with the nonlinear stiffness (ModNoFrict). This was not true for the frequency, for large motion amplitudes the frictional forces implemented in the investigated models no longer seem to influence the frequencies significantly.

5.3 Sources of lead-lag motion damping for the considered rotor

Damping in helicopter rotors can have multiple sources:

- Discrete lead-lag dampers (in this rotor the frictional characteristics of the loop attachment)
- Structural damping of elastic blade bending
- Aerodynamic forces

In section 5.2, it was shown that the use of the frictional reduced order model leads to higher damping ratios for the cases where damping was low for the baseline

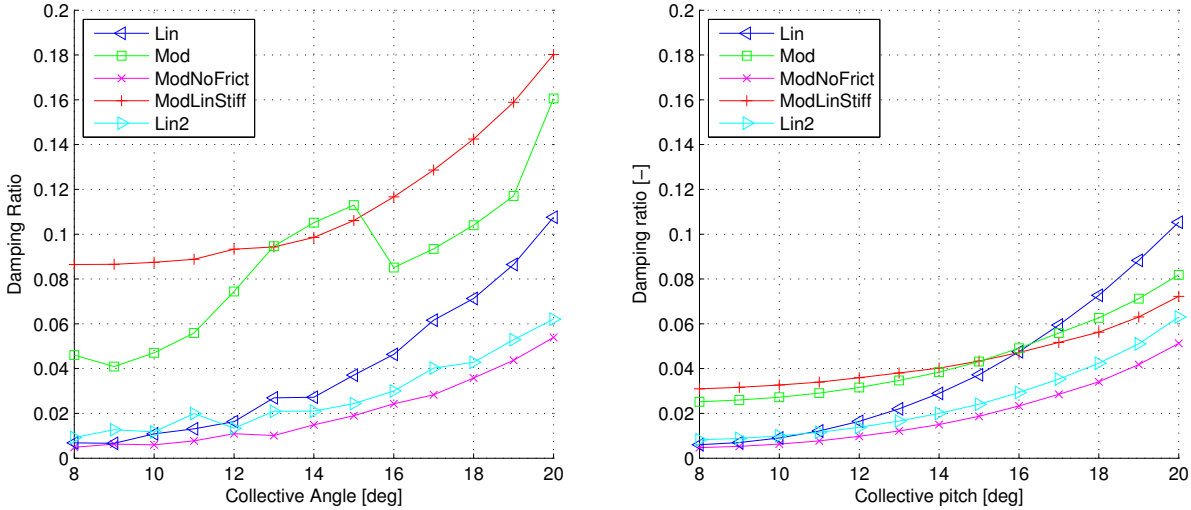

(a) Small amplitude motion (F=150N)

(b) Large amplitude motion (F=1000N)

Figure 20: Damping ratio for the in-plane motion

model, a favorable property since a stability margin has to be provided for all operating conditions of a helicopter rotor. Generally, a hingeless helicopter blade constitutes a highly coupled system which is very sensitive to blade root boundary conditions. Because the proposed reduced order model does not only introduce a frictional element but is also shown to change the blade motion as a whole, it is not inherently clear which mechanism is responsible for the increase in damping. However, when looking at the results for the different blade configurations in conjunction, the following conclusions may be drawn for the studied model:

- A reduction of stiffness in the direction of the airfoil causes a significant drop in oscillation frequency and results in a weaker coupling between lag and flap motion. Eventually, the latter leads to reduced aerodynamic damping.
- For small motion amplitudes the frictional forces in the model are large enough to influence in-plane oscillation frequency, for larger amplitudes of motion this is not the case (Mod vs. ModNoFrict in Figs. 19 a and b)
- The frictional forces generate damping for small and large amplitudes of motion (Mod and ModLinStiff in Figs. 19 a and b), although the effect is weaker for large motion amplitudes.
- The amount of damping generated by frictional forces is dependent on how freely the frictional joint can move (Mod vs. ModLinStiff in Fig. 20 a)
- The nonlinear stiffness of the ROM does not have beneficial effects on damping when considered independent from friction (Mod vs. ModNoFrict in Figs. 19 a and b).

To clarify further to what extend the frictional damping contributes to the overall damping of the system, the energy dissipated in the two discrete frictional elements of the ROM is considered. The absolute energy values have to be put into context for interpretation. For this reason, the force displacement relationship for the in-plane tip force has been used to estimate the difference in potential energy of the trim state and the static deflected state prevalent at the beginning of the oscillatory motion just before the force is released. When the blade oscillation has decayed, this energy has been dissipated due to the above named physical sources. This reasoning is true for real life technical systems, but not necessarily for the trajectories obtained from the simulation models used in this work as the time marching integration algorithm used is not energy preserving. Although plausible, the results in this section have to be treated with care for this reason and rather have indicative than quantifying character.
Figure 21 shows the ratio of the cumulated energy dissipated in the frictional elements of the model and the estimated potential energy of the initially deflected blade. Thus, it provides a good idea to what extend the frictional characteristics contribute to the overall damping of the in-plane motion. For the full reduced order model the confined increase in damping for small amplitude motion and pitch angles between 12° and 15° from Fig. 20 is matched by an increase in dissipated frictional work share. In general, collective pitch angle elevation comes with a reduced share of frictional dissipation. As the airfoil is inclined, aerodynamic forces are tilted and a larger and larger component acts in the in-plane direction resulting in higher damping of

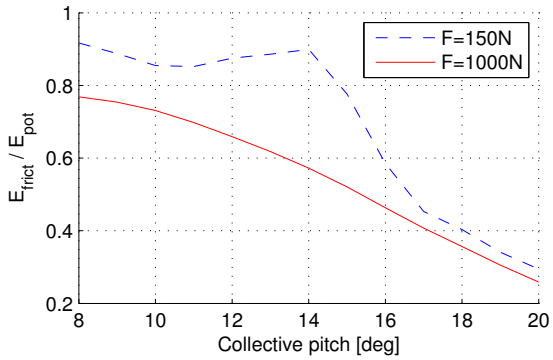

Figure 21: Ratio of frictional work and initial potential energy

the lead-lag motion. Furthermore, for higher pitch angles the in-plane motion is more and more performed through bending about the elastic axis perpendicular to the joint axis due to the mechanical setup of the rotor system. For small amplitude motion the model of the full ROM predicts that between 80 % and 90 % of the potential energy is dissipated by means of friction for a range from 8° to 14° of collective pitch angle. For higher pitch angles, this share is reduced dramatically. For large amplitudes of motion the share in energy dissipation declines for all trim conditions because the rotation in the joint of the ROM does not grow with the blade tip amplitude due to the nonlinear stiffness in the model. Also, frictional Coulomb forces are saturated in magnitude. These mechanisms might help to prevent overheating of the blade loop in operating conditions. The results shown in Fig. 21 support the hypothesis that the damping advantage for the augmented model is caused by friction rather than by a more favorable aeroelastic setup due to changed boundary conditions of the blade.

6 CONCLUSION

- An entirely new rotor analysis model has been set up in the Modelica language and its capability for dynamical analysis has been shown.
- A loop-type blade attachment similar to the one used in the MBB Bo105 / EC145 has been modeled with 3D finite elements in ANSYS with special regard on the frictional contact surface. Using preexisting test data, the model has been parameterized and validated.
- Finite element simulations enabled the setup of a simple reduced order model suitable for dynamical rotor analysis. The suggested ROM for the blade loop attachment features backlash and Coulomb friction occuring at a single revolute joint.
- Inserting the proposed ROM into a hingeless rotor model, it was found that it reduces the lag-flap coupling of the rotor design under consideration when compared to a clamped blade. Since special emphasis has been put on the stabilizing properties of elastic coupling in previous investigations[5], the blade loop attachment may come with a detrimental effect in this regard.
- A fundamental change in oscillation mechanism due to stick-slip behavior is discovered for very small oscillation amplitudes only. For the onset of a potential instability, small amplitude behavior may be designated as very important. On the other hand, the helicopter blade faces ongoing lag motion due to asymmetric flow conditions, cyclic pitch and flapping as well as vibrations which may prevent the occurrence of sticking altogether.
- The proposed ROM acts as a damper. Depending on the trim condition and the amplitude of a lead lag oscillation the ROM dissipated from 30 % up to 90 % of the energy necessary to damp out the blade motion. For the operating states examined, the damping advantage of the models featuring the frictional model can be attributed to the frictional dissipation itself rather than to a more favorable aeroelastic coupling induced by the modified mechanics.
- Beforehand, it was not clear to what extend the stick-slip model affects blade motion. That is why a reduced order model was developed and the behavior of the coupled system has been studied. Severe couplings between the changing boundary condition and elastic blade deformation have been shown to occur. However, for the parameterization of the model investigated in this paper, these couplings only become relevant in special conditions.

  The friction model only alters oscillation frequency for small amplitudes. Besides, it was found that for a large range of motion amplitudes, the fundamental oscillation is carried out in a similar manner with regard to elastic couplings. This was due to the low coefficient of friction, preventing sticking for many operating states. For this reason, it should be feasible to describe the blade dynamics found herein with a model using a modified stiffness and a damper model without the stick-slip property. Of course, for the damper, a parameterization dependent on operating state will be necessary. Such a model may enable stability analysis by means of linearization. For a different parameterization of the model, sticking might occur more frequently and what was stated above may no longer be true.
- The analysis presented herein is considered suitable for low frequency blade dynamics since this is easily provoked by external excitation. A time

domain analysis as the one performed here for analyzing high frequency blade dynamics may be cumbersome or even inadequate.

- Further experimental study on the considered system is required to compare the mechanisms and results predicted herein to test data.

The analysis reveals that the nonlinear blade attachment under investigation has significant effects on the fundamental lead-lag dynamics. These effects are neglected in conventional eigenvalue analysis but have to be studied to arrive at valid simulation models. For certain operating conditions, accurate modeling of a stick-slip nonlinearity might be of utmost importance for the prediction of critical dynamical behavior such as air and ground resonance.

ACKNOWLEDGEMENTS

This work was supported by Airbus Helicopters providing relevant data and helpful comments – namely: Oliver Dieterich, Peter Konstanzer, Jean-Baptiste Maurice and Dieter Wierer. Many thanks also go to Olivier A. Bauchau, Simon Radler and Christian Spieß for fruitful discussions. Associated with their master theses projects, Willem Garre and Verena Heuschneider greatly contributed to the overall progress by developing model evaluation routines and performing parametric studies.

7 REFERENCES

[1] Olivier A. Bauchau, Yannick Van Weddingen, and Sandeep Agarwal. “Semiactive coulomb friction lead-lag dampers”. In: *Journal of the American Helicopter Society* 55 (2010). DOI: 10.4050/JAHS.55.012005.

[2] William G. Bousman. “An experimental investigation of the effects of aeroelastic couplings on aeromechanical stability of a hingeless rotor helicopter”. In: *Journal of the American Helicopter Society* 26.1 (1981), pp. 46–54.

[3] H. Elmqvist, F. E. Cellier, and M. Otter. “Object-oriented modeling of hybrid systems”. In: *Proc. ESS 93 European Simulation Symposium*. (Delft, Netherlands). Oct. 1993.

[4] Farhan Gandhi and Inderjit Chopra. “Analysis of bearingless main rotor aeroelasticity using an improved time domain nonlinear elastomeric damper model”. In: *Journal of the American Helicopter Society* (1996), pp. 267–277.

[5] Helmut B. Huber. “Effect of torsion-flap-lag-coupling on hingeless rotor stability”. In: *Proc. 29th Annual National Forum of the American Helicopter Society*. (Washington). May 1973.

[6] Wayne Johnson. “Influence of unsteady aerodynamics on hingeless rotor ground resonance”. In: *Journal of Aircraft* 19.8 (1982), pp. 668–673.

[7] Wayne Johnson. “Rotorcraft dynamics models for a comprehensive analysis”. In: *Proc. 54th Annual National Forum of the American Helicopter Society*. (Washington). May 1998, p. 1207.

[8] Holger Kolsch. *Schwingungsdaempfung durch statische Hysterese*. VDI Fortschrittsberichte. VDI Verlag, 1993. ISBN: 3-18-149011-3.

[9] Vincenzo Muscarello and Guiseppe Quaranta. “Multiple input describing function for non-linear analysis of ground and air resonance”. In: *Proc. 37th European Rotorcraft Forum*. (Gallarate, Italy). Sept. 2011, Paper No. 111.

[10] David A. Peters and Ninh Ha Quang. “Technical note: Dynamic inflow for practical applications”. In: *Journal of the American Helicopter Society* 33.4 (1988), p. 64.

[11] D. M. Pitt and D. A. Peters. “Rotorcraft dynamic inflow derivatives and time constants from various inflow models”. In: *Proc. 9th European Rotorcraft Forum*. (Stresa, Italy). Sept. 1983, Paper No. 55.

[12] Christian Spieß and Manfred Hajek. “A Modelica library of anisotropic flexible beam structures for the simulation of composite rotor blades”. In: *Proc. 9th International Modelica Conference*. (Munich). Sept. 2012, pp. 161–174. DOI: 10.3384/ecp12076417.

[13] B. H. Tongue. “Response of a rotorcraft model with damping nonlinearities”. In: *Journal of Sound and Vibration* 103.2 (1985), pp. 211–224.